





Article

Islanding Detection with Reduced Non-Detection Zones and Restoration by Reconfiguration

Sowmya Ramachandradurai ¹, Narayanan Krishnan ^{2,*}, Gulshan Sharma ^{3,*} and Pitshou N. Bokoro ³

¹ Department of Electrical and Electronics Engineering, Sri Shakthi Institute of Engineering & Technology, Coimbatore 641062, India

² Department of Electrical and Electronics Engineering, SASTRA Deemed to be University, Thanjavur 613401, India

³ Department of Electrical Engineering Technology, University of Johannesburg, Johannesburg 2006, South Africa

* Correspondence: narayanan.mnit@gmail.com (N.K.); gulshans@uj.ac.za (G.S.)

Abstract: The development and use of PV (Photovoltaic), Wind, and Hydro-based Distributed Generation (DG) is presently on the rise worldwide for improving stability and reliability, and reducing the power loss in the distribution system with reduced emission of harmful gases. A crucial issue addressed in this article, due to the increased penetration of DGs, is islanding operations. The detection of islanding is performed by a proposed v&f (voltage and frequency) index method. The reliability indices of the IEEE-33 and 118 radial bus distribution system after the detection of islanding by the proposed method is evaluated by considering the islanding issue as customer interruption. To mitigate the islanding, a reconfiguration strategy using Particle Swarm Optimization (PSO) is also performed and the proposed strategy is also evaluated with the conventional reconfiguration strategy of the distribution system.

Keywords: distributed generation (DG); v&f (voltage and frequency) index; particle swarm optimization (PSO); reconfiguration; reliability; ENS; ASAI; AENS; SAIDI; SAIFI



Citation: Ramachandradurai, S.; Krishnan, N.; Sharma, G.; Bokoro, P.N. Islanding Detection with Reduced Non-Detection Zones and Restoration by Reconfiguration. *Energies* **2023**, *16*, 3035. <https://doi.org/10.3390/en16073035>

Academic Editors: Vinicius Jacques Garcia and Daniel Pinheiro Bernardon

Received: 8 February 2023

Revised: 14 March 2023

Accepted: 20 March 2023

Published: 27 March 2023



Copyright: © 2023 by the authors. Licensee MDPI, Basel, Switzerland. This article is an open access article distributed under the terms and conditions of the Creative Commons Attribution (CC BY) license (<https://creativecommons.org/licenses/by/4.0/>).

1. Introduction

Distributed Generation (DG) units have attracted more observation from researchers due to the high cost of new power plants, increasing electricity demand, and depleting fossil fuels. DG installation reduces the necessity for grid reinforcement and power losses. The presence of DGs in a radial network changes the voltage magnitude and current. The change in voltage magnitude and current impacts on the operation of protection relays are studied in [1–3]. Unintentional islanding is an important problem, which leads to damage to consumer appliances [4,5]. Detection of unintentional islanding can be performed by using the remote method and local methods. The remote method requires a communication signal to detect the islanding, whereas the local method detects islanding without the communication signal [6,7].

The voltage, frequency, and current on the distribution side are measured to detect islanding using the passive method [5,8]. In the active method, internal disturbances are created in the network to detect the islanding based on the system response [9–11]. Combining the advantages offered by active and passive methods, hybrid methods have been devised by researchers [12]. The Non-Detection Zones (NDZ) are eliminated in the active method but induce power quality issues, and islanding is not detected when the system is connected with multiple inverters. The NDZ is represented as the failure of detection of islanding events in the system. Therefore, the passive islanding detection method is used to detect the islanding with reduced power quality issues connected with multiple inverters [13,14].

In power loss, islanded buses can be reduced and reliability can be improved by network reconfiguration. The sectionalizing lines and tie lines are the two lines present in the distribution system, where the tie lines are opened lines and sectionalizing lines are closed lines. The change of position of sectionalizing and tie-line switches is achieved by network reconfiguration [3,8]. The reliability indices in the distribution system can be evaluated through customer interruptions. The continuity of power becomes a major competitive factor for grid operators. Therefore, the evaluation of reliability indices is very much important in the distribution system [15–17].

The indices are evaluated by sensitivity analysis. This can be divided into two methods: the perturbation method [18], where no analytical calculation is required, and the partial derivative method [19], which involves analytical calculation [20,21]. The improvement in reliability is performed by improving the energy efficiency performance index. The reliability indices such as System Average Interruption Duration Index (SAIDI), System Average Interruption Frequency Index (SAIFI), and Energy Not supplied (ENS) are evaluated with a network reconfiguration using the mixed-integer linear programming method [22,23].

Contributions of the Proposed Method

The present work deals with passive islanding detection in the presence of various DGs using the BFS (Backward and Forward Sweep) method along with network reconfiguration using the PSO (Particle Swarm Optimization) technique. The islanding is detected by measuring the voltage and frequency (v&f) values simultaneously with fixed threshold limits. The reliability indices such as SAIFI, ENS, SAIDI, AENS (Average Energy Not Supplied), and ASAI (Average System Availability Index) are evaluated by considering the islanding issue as an interruption to the system before reconfiguration and after reconfiguration. The results are validated for the IEEE-33 and 118 bus systems.

- The Non-Detection Zones, the number of islanded buses and detection time are reduced by the proposed technique.
- A PSO technique is used to perform the reconfiguration by considering the identified vulnerable buses for islanding by the proposed islanding detection method.
- Reliability indices are evaluated for the proposed reconfigured system.
- The Real Time Price (RTP) and time of use are not considered in this work. In future, the interruption cost or feasibility studies can be implemented through the cost of electricity based on RTP.

2. Passive Method for Detection of Islanding, Reconfiguration, and Reliability Evaluation

A passive islanding detection method is proposed to detect islanding by measuring the voltage and frequency variation in the radial distribution system. The reliability values are evaluated before and after reconfiguration to prove the network operation is reliable.

2.1. Proposed Voltage and Frequency (v&f) Variation Technique

The DGs, such as PV (Photovoltaic), Wind, and Hydro are used in proposed method to enhance the reliability with lower losses and also reduces the pollution.

2.1.1. PV

Solar energy converted to electric current is called the PV effect. The solar panels absorb the sunlight. It is an abundant source of energy, and it is a clean and sustainable source of energy. The cost is higher during the starting stage of usage and the cost is reduced gradually with increased efficiency. The power generation depends on solar insolation, the atmospheric temperature, and also the rating of the module itself. The PV output power is given as follows [24]:

$$O_{Power(PV)} = N_{pan} \times F_{fact} \times V_{Pan} \times I_{Pan} \quad (1)$$

$$F_{fact} = \frac{V_{MNPO} \times I_{MNPO}}{V_{ope} \times I_{Shcc}} \quad (2)$$

$$V_{pan} = V_{ope} - C_{volt} \quad (3)$$

$$I_{pan} = SOIR[I_{Shcc} + K_{curnt}(T_{spc} - 25)] \quad (4)$$

$$T_{spc} = T_{amb} + SOIR[(T_{oper} - 20)/0.8] \quad (5)$$

The values calculated for PV modeling are explained in Table 1.

Table 1. Parameters of PV.

Variables [24]	Ratings
The Maximum Net Power Output (MNPO) current, I_{MNPO}	4.76 A
The Maximum Net Power Output (MNPO) voltage, V_{MNPO}	17.32 V
The voltage coefficient, C_{volt}	14.40 mV/°C
Optimal temperature, T_{oper}	43 °C
The current coefficient, K_{curnt}	1.22 mA/°C
Open circuit voltage, V_{ope}	21.98 V
Short circuit current, I_{Shcc}	5.32 A

$O_{Power(PV)}$ —Output power of PV, F_{fact} —Fill factor, SOIR- Solar Irradiation of PV model, T_{spc} —Particular solar cell temperature and T_{amb} —Ambient temperature of PV, V_{pan} —Voltage at the particular panel, I_{pan} —Current at the particular panel and N_{pan} —No of panels, respectively, [24].

2.1.2. Wind

The wind turbine produces power which is not constant and varies from seconds to seconds, because the turbine speed is not constant. Therefore, the wind power generation profile units are affected due to the intermittency of the wind speed. Modeling of wind speed is framed by the Weibull Probability Distribution Function (PDF). The wind output power is given as follows [24]:

$$W_{pow} = \begin{cases} 0, & V \leq C_{in}^{sp} \text{ or } V \geq C_{out}^{sp} \\ \frac{V - C_{in}^{sp}}{S_{rat} - C_{in}^{sp}} W_{rpow}, & C_{in}^{sp} \leq V \leq S_{rat} \\ W_{rpow}, & \text{else} \end{cases} \quad (6)$$

The values calculated for Wind modeling are explained in Table 2.

Table 2. Parameters of Wind.

Variables [24]	Ratings
Power (Rated), W_{rpow}	0.5 MW
Rated speed, S_{rat}	13 m/s
Speed (cut in), C_{in}^{sp}	3 m/s
Speed (cut out), C_{out}^{sp}	25 m/s

2.1.3. Hydro

The Hydro energy system requires more space and cost but has very low emissions. Conversion of kinetic energy into electrical energy is executed in the Hydro energy system. It is considered to be a dispatchable generation unit and the hydro power output is given as follows [25]:

$$H_{Pow} = \epsilon_{Hy} \times \rho \times g_{ac} \times P_{he} \quad (7)$$

The values calculated for hydro modeling are explained in Table 3.

Table 3. Parameters of Hydro.

Variables [25]	Ratings
Hydraulic efficiency, ϵ_{Hy}	75.1%
Density, ρ	1000 Kg/m ³
Effective pressure, P_{he}	2.25 m
acceleration, g_{ac}	9.81 m/s ²

The proposed method of v&f is modeled as follows:

$$M_1 = S_2/b_V \text{ and } M_2 = S \times V_{ch} \quad (8)$$

$$S_2 = \sum_1^{3353} (1/N_{smpl} \times abs(S_1)) \quad (9)$$

$$S_1 = \sum_1^{3353} (volt)_{mag} \sin 2\pi N_{smpl} f t \quad (10)$$

$$V_{ch} = b_V - V_{operating(N)} \times S_2 \quad (11)$$

$$V_{operating(N)} = b_V - V_{operating} \quad (12)$$

$$S = \int_0^n (f_{ch} \times 2\pi) / 60 \quad (13)$$

$$f_{ch} = 60 - D_{fr} \quad (14)$$

$$D_{fr} = 1 + f \times [(P_{lo(n)} / P_{alo(n)}) \times (b_V / V_{operating})] \quad (15)$$

Table 4 shows the variables and ratings of 33 and 118 test systems, which are evaluated by the above equations. The change of frequency at a bus concerning system frequency is calculated by Equation (13). The summation is taken for the number of samples related to phase voltage as expressed in Equation (9); the product of the number of samples, frequency, time with voltage magnitude are expressed in Equation (10). The change in voltage is calculated through taking the difference between the base voltage and operating voltage, as expressed in Equation (11). The new operating voltage of each bus is determined to measure the change in voltage (V_{ch}) through Equation (12). If $M_1 > M_2$ islanding is occurred in a particular bus which is determined with Equation (8) and loads in all buses are varied simultaneously at each hour. Accordingly, the samples/cycle is changed in all the buses. The proposed detection method is compared with two different existing methods. The first existing method [26] uses a change in voltage and the second existing method [27] uses a change in frequency.

Table 4. Parameters of proposed method.

Variables	Ratings (33 Bus System)	Ratings (118 Bus System)
M_1 and M_2 —v&f index and threshold limits	0.09684 and 0.10504	0.099243 and 0.2432
S_1 and S_2 —The phase voltage related to time, frequency and voltage	1.5925 and 1.226	1.6251 and 1.426
$P_{lo(n)}$ —(Real power) difference between first bus to next bus	7.2 kW	9.3 kW
$P_{alo(n)}$ —Actual load	20 kW	23 kW
N_{smp} —Samples (Range)	3335	3335
$V_{operating(N)}$ —Operating voltage new	11.66 kV	9 kV
$V_{operating}$ —Operating bus voltage	0.995 kV	0.997 kV
b_V —Voltage (base)	12.66 kV	11 kv
f_{ch} —Change in (f)-frequency	0.36 Hz	0.39 Hz
V_{ch} —Change in voltage	1.226 kV	1.121 kV
D_{fr} —Calculated frequency	59.64 Hz	59.61 Hz
n—Number of buses	33	118

2.2. Reconfiguration Using Particle Swarm Optimization (PSO) Technique

Reconfiguration is performed with three rules to verify the radial mode at each stage as follows [28]:

Rule 1: Every candidate switch must belong to its corresponding loop vector.

Rule 2: A single candidate switch alone is chosen from one common branch vector.

Rule 3: All the common branch vectors of a prohibited group vector cannot participate simultaneously to form an individual.

Rule 1, Rules 2, and Rule 3 prevent islanding of exterior, interior, and principle interior nodes. These rules ensure a feasible radial mode.

The objective is resolved with the equality and inequality constraints. The best personal solution is obtained for each and every iteration. Finally, the best global solution is identified by best personal solution [29].

$$G_b = \min [P_{be}^t] \text{ or } \max [P_{be}^t] \quad (16)$$

$$P_{be}^{t+1}, i = \begin{cases} P_{be}^{t+1}, & \text{if } F(y_i^{t+1}) > P_{be,i}^t \\ y_i^{t+1}, & \text{if } F(y_i^{t+1}) \leq P_{be,i}^t \end{cases} \quad (17)$$

$$VE_{ij}^{t+1} = VE_{ij}^t + K_1 r_{1j}^t [P_{be,i}^t - (y_{ij}^{t+1})] \quad (18)$$

The proposed particle or switch selection can be written as,

$$y^t = S_1, S_2, S_3, \dots, S_\beta, T_{g1}, T_{g2}, \dots, T_{g\alpha} \quad (19)$$

$$\omega(t+1) = \frac{\omega_{\max} - \omega_{\min}}{t_{\max}} \times t \quad (20)$$

where G_b represents the best global solution and $P_{(be)}$ represents the best personal solution, which are calculated using particle velocity V_{ij} , fitness value, or objective function 'F'

and the specific place of the particle y_i^{t+1} , acceleration (K_1) constant and r_{1j}^t —random numbers [29].

Opened switches are represented by T_g as the variable and ‘S’ are represented as closed switches, α and β are represented as tie line and number of DG, ω_{max} and ω_{min} are maximum and minimum inertia weight, t_{max} and t_{min} are complete number of iterations and present iteration, respectively. The better solution of the system is identified by reconfiguring or rearranging the network to attain the desired improvement in an index. The procedure for reconfiguration using PSO is as follows [29]:

- 1: The switches will open after the initialization of particles and checking the system working in radial behavior.
- 2: The number of velocity (particle) and switches (opened) are randomly generated.
- 3: The random particle generation and switches (closed) are performed by choosing the proper configuration.
- 4: The best and fitness values of every particle choose the appropriate (particle best) value.
- 5: The iterations are made to notify the accurate switches for performing the reconfiguration by best values, the velocity values, place of the particles from Equations (17)–(19).
- 6: In the last stage, the switches are opened as the best global solution.

2.3. Proposed Method for Reliability Evaluation

The indices, such as (ENS)—Energy Not Supplied, (ASAI)—Average System Availability Index, (AENS)—Average Energy Not Supplied, (SAIFI)—System Average Interruption Frequency Index, and (SAIDI)—System Average Interruption Duration Index, are identified by the following equations.

$$\text{SAIDI} = \frac{\sum_j h_j * n_j}{\sum_j n_t} \quad (21)$$

$$\text{SAIFI} = \frac{\sum_j \lambda_j * n_j}{\sum_j n_t} \quad (22)$$

$$\text{ENS} = L_{b(j)} * h_j \quad (23)$$

$$\text{AENS} = \frac{\text{ENS}}{n_t} \quad (24)$$

Here, n_j —customer interruption or customer not served, h_j —customer hours for available services, failure rate is denoted as λ_j , n_t —total number of customers served and total demand is represented as $L_{b(j)}$.

Figure 1 represents, in the proposed work, all the bus systems considered with detection of islanding as an interruption. Load flow is performed by increasing the load profile linearly using the Backward and Forward Sweep (BFS) method from base load of the network to 130% of base load. An operating voltage of all the buses are measured, and the variation of v&f index and threshold values are measured using Equation (8). The violation limits are examined with $\pm 2\%$ of voltage and frequency values using IEEE std. 1547 [30]. If v&f variation values are higher than the values of threshold limits then that specific bus is considered to be an islanded bus. Along with the determined islanded bus, a strategy of reconfiguration is undertaken to confirm the continuity of the supply. A quantitative indices evaluation is performed before and after reconfiguration to estimate the outcome of strategy of reconfiguration in the network.

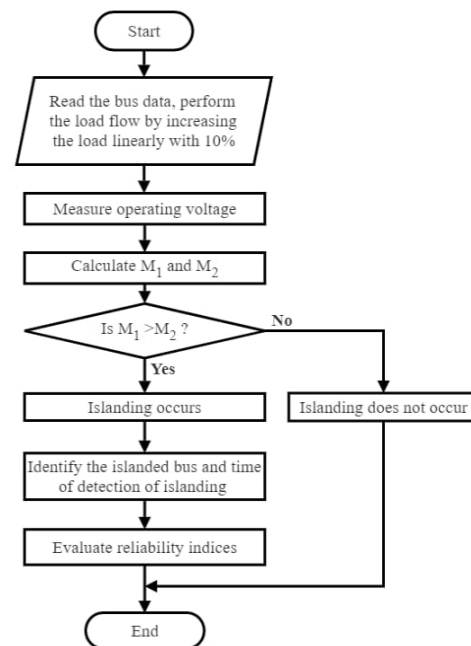


Figure 1. Flowchart using v&f index variation method for islanding detection with reconfiguration and reliability evaluation.

3. Results and Discussion

Renewables such as PV, Wind, and Hydro-based DGs installed in all distribution systems reduce the loss and increase the stability which is simulated through MATLAB-2016b [31]. The loads are varied linearly in steps of 10% of base load to 130% of base load for detection of islanding by the proposed passive method of simultaneous measurement of voltage and frequency for both 33 and 118 bus system. The proposed islanding detection method is compared with the existing methods.

3.1. Islanding Detection

The islanding is performed for the IEEE-33 and 118 bus radial system and results obtained by the proposed technique are compared with existing methods.

3.1.1. Islanding Detection for the 33 Bus System

The 33 bus system under consideration is shown in Figure 2. The buses 14, 24, and 29 are installed as PV with the rating of 691 kW, 986.1 kW, and 1277.3 kW, respectively [32]. The buses 14 and 30 are installed as Wind with the rating of 722.56 kW and 813.89 kW, respectively [33]. The buses 13, 24, and 30 are installed as Hydro with the rating of 537.8 kW, 1058.9 kW, and 967.7 kW, respectively [32].

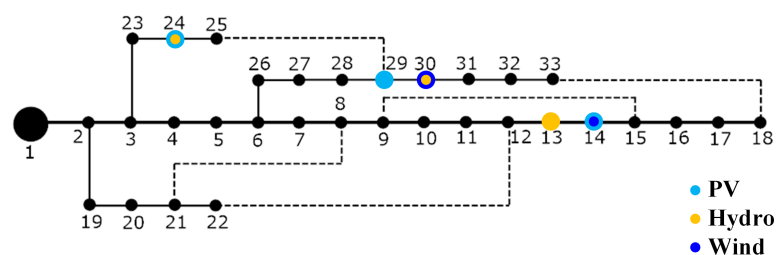


Figure 2. Electrical bus system-33.

Table 5 shows the outcome of the two existing methods with the proposed method for various DG units. The time of detection is determined by the change in voltage and change in frequency at an islanded bus. The loads in various DG combinations are not changed until 0.5 s. After 0.5 s, the loads in all DGs are linearly increased.

Table 5. Comparison results of islanding detection for the 33 bus system.

DGs	Buses	Islanding Detection								
		Voltage Based Method [26]			Frequency Based Method [27]			Proposed Passive Method (Simultaneous Measurement of v&f Variation)		
		Islanded Bus No	No of Buses Islanded	Time of Detection (Seconds)	Islanded Bus No	No of Buses Islanded	Time of Detection (Seconds)	Islanded Bus No	No of Buses Islanded	Time of Detection (Seconds)
PV	14, 24, 29	24, 29	7	1.29	14, 24, 29	10	1.95	24	2	1.02
Wind	14, 30	14, 30	9	0.99	14, 30	9	0.98	14	5	0.75
Hydro	13, 24, 30	13, 30	10	0.82	24, 30	6	0.65	24	2	0.60
PV-Hydro	13, 14, 24, 29, 30	14, 24, 30	11	1.054	13, 29	11	1.032	24	2	0.75
PV-Wind	14, 24, 29, 30	14, 24, 30	11	0.62	14, 30	9	0.88	14	5	0.58
Wind-Hydro	31, 14, 24, 30	14, 24, 30	11	1.98	14, 30	9	1.99	24	2	0.75

While increasing the profile of load, there is a sudden distortion in voltage and frequency at 1.02 s—(PV), 0.75 s—(Wind), 0.6 s—(Hydro), 0.75 s—(PV-Hydro), 0.58 s—(PV-Wind), and 0.75 s—(Wind-Hydro). In the presence of PV, the proposed methodology noticed islanding at the 24th bus at 114.6% of the base load itself. However, by existing methods [26,27], the islanding is noticed at base loads of 116.1% and 129.3%.

In the presence of Wind, the proposed method noticed islanding at 14th bus at 113.1% of the base load itself. However, by existing methods [26,27], the islanding is detected at base loads of 114.3% and 119.2%.

In the presence of Hydro, the proposed method noticed islanding at the 24th bus at 111.9% of the base load itself. However, by existing methods [26,27], the islanding is noticed at base loads of 129.7% and 112.9%.

In the presence of PV-Hydro, the proposed method noticed islanding at the 24th bus at 113.4% of the base load itself. However, by existing methods [26,27], the islanding is noticed at base loads of 124.4% and 124.2%.

In the presence of PV-Wind, the proposed method noticed islanding at the 14th bus at 111.7% of the base load itself. However, by existing methods [26,27], the islanding is noticed at base loads of 112.6% and 129.9%.

In the presence of Wind-Hydro, the proposed method noticed islanding at the 24th bus at 113.4% of the base load itself. However, by existing methods [26,27], the islanding is noticed at the base load of 130%.

In the proposed v&f index (passive islanding) method, voltage and frequency are monitored regularly, M_1 and M_2 are calculated for different DGs from Equation (8). The islanding is detected mostly at the 24th bus. This is because the larger generation in the bus leads to violation of the frequency limits.

Figure 3a,b represents the voltage and frequency deviation of buses in the presence of various distributed generation units. Buses in which the threshold crossed from the fixed voltage (0.99 to 1.05 p.u.) and fixed frequency ($\pm 2\%$ of the rated frequency) were considered to be islanded buses. Figure 4 has '0' and '1' which denotes the islanded bus and non-islanded bus, respectively.

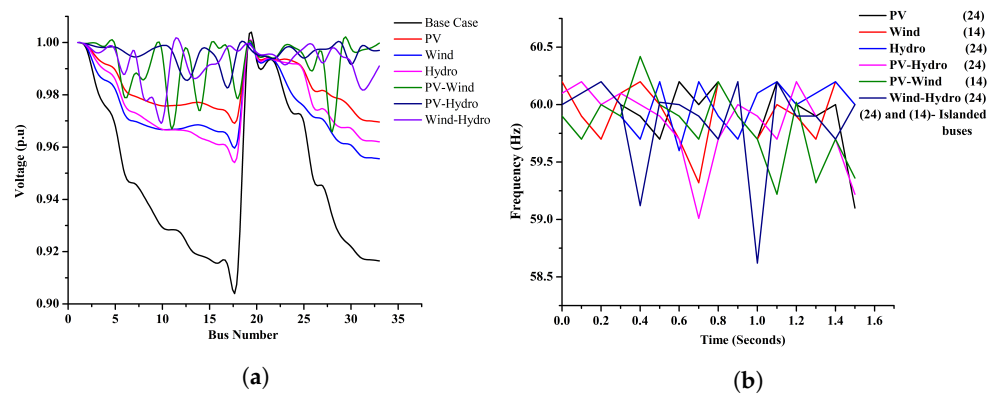


Figure 3. Voltage and frequency values. (a) Values (Voltage)- 33 bus system. (b) Values (Frequency)- 33 bus system.

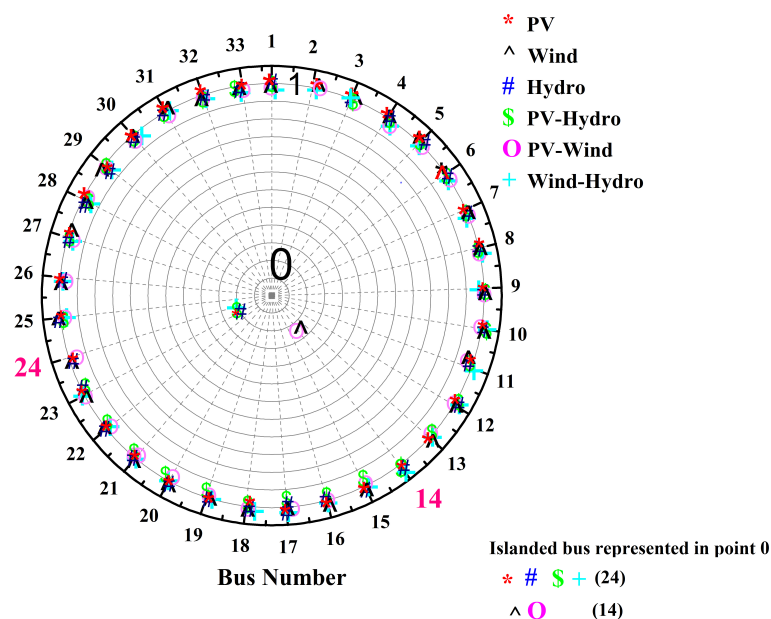


Figure 4. Detection of islanded buses- 33 bus system.

3.1.2. Islanding Detection for the 118 Bus System

The 118 bus system under consideration is shown in Figure 5. The buses 20, 30, 47, 73, 80, 90, and 110 are installed as PV with the rating of 2.0856 MW, 3.3381 MW, 2.1249 MW, 2.794 MW, 2.0369 MW, 2.6069 MW, and 3.1877 MW, respectively [34]. The buses 2, 5, 12, 44, 53, 82, and 86 are installed as Wind with the rating of 2.1 MW, 1.7 MW, 1.65 MW, 2 MW, 1.55 MW, 1.85 MW, and 1.95 MW, respectively [35]. The buses 20, 39, 47, 74, 85, 90, and 110 are installed as Hydro with the rating of 2.0187 MW, 3.2905 MW, 2.0615 MW, 2.4092 MW, 1.7437 MW, 2.5473 MW, and 3.1775 MW, respectively [34].

Table 6 shows comparison results of two existing methods with the proposed method for various DG units. The time of detection is determined by the change in voltage and change in frequency at an islanded buses. The loads in various DG combinations are not changed until 0.5 s. After 0.5 s, the loads in all DGs are linearly increased.

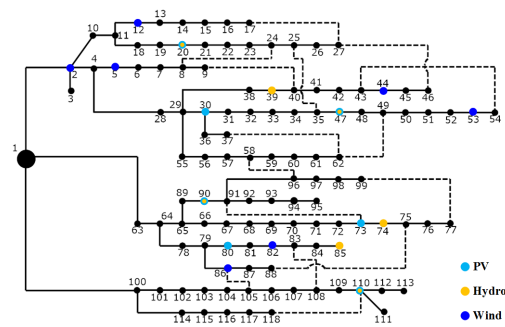


Figure 5. Electrical bus system-118.

Table 6. Comparison results of islanding detection for the 118 bus system.

DGs	Buses	Islanding Detection								
		Voltage Based Method [26]			Frequency Based Method [27]			Proposed Passive Method (Simultaneous Measurement of v&f Variation)		
		Islanded Bus No	No of Buses Islanded	Time of Detection (Seconds)	Islanded Bus No	No of Buses Islanded	Time of Detection (Seconds)	Islanded Bus No	No of Buses Islanded	Time of Detection (Seconds)
PV	20, 39, 47, 73, 80, 90, 110	47, 80	14	1.39	80, 110	10	1.59	110	4	1.25
Wind	5, 82, 86	5, 82, 86	12	1.75	5, 86	8	1.32	5	5	1.30
Hydro	39, 47, 110	39, 47, 110	20	1.55	39, 110	12	1.55	110	4	1.50
PV-Hydro	20, 80, 90, 110	80, 110	10	1.92	80, 110	10	1.99	110	4	1.79
PV-Wind	5, 39, 44, 47, 82	5, 39, 82	22	0.59	5, 82	9	0.75	5	5	0.55
Wind-Hydro	74, 82, 86, 110	86, 110	7	1.99	86, 110	7	0.99	110	4	0.93

While increasing the profile of load there is a sudden distortion in voltage and frequency at 1.25 s—(PV), 1.30 s—(Wind), 1.50 s—(Hydro), 1.79 s—(PV-Hydro), 0.55 s—(PV-Wind) and 0.93 s—(Wind-Hydro).

In the presence of PV, the proposed method noticed islanding at the 110th bus at 114.9% of the base load itself. However, by existing methods [26,27], the islanding is noticed at base loads of 120.9% and 123.5%.

In the presence of Wind, the proposed method noticed islanding at the 5th bus at 112.5% of the base load itself. However, by existing methods [26,27], the islanding is noticed at base loads of 128.3% and 114.7%.

In the presence of Hydro, the proposed method noticed islanding at the 110th bus at 120.3% of the base load itself. However, by existing methods [26,27], the islanding is noticed at a base load of 125.9%.

In the presence of PV-Hydro and Wind-Hydro, the proposed method noticed islanding at the 110th bus at 128.7% (PV-Hydro) of base load and 111.3% (Wind-Hydro) of base load. However, by existing methods [26,27], the islanding is noticed at base loads of 129.5% and 130% for PV-Hydro, and 112% and 113.4% for Wind-Hydro.

In the presence of PV-Wind, the proposed method noticed islanding at the 5th bus at 113.6% of the base load itself. However, by existing methods [26,27], the islanding is noticed at base loads of 130% and 124.3%.

In the proposed v&f index (passive islanding) method, voltage and frequency are monitored regularly, M_1 and M_2 are calculated for different cases of DGs from Equation (8). The islanding is noticed mostly at the 110th bus. This is because the larger generation or load in the bus leads to violation of the frequency limits.

Figure 6a,b denotes the voltage and frequency deviation of buses in the presence of various distributed generation units. Buses in which the threshold crossed from the

fixed voltage (0.99 to 1.05 p.u.) and fixed frequency ($\pm 2\%$ of the rated frequency) were considered to be islanded buses. Figure 7 has '0' and '1', which represent the islanded bus and non-islanded bus, respectively.

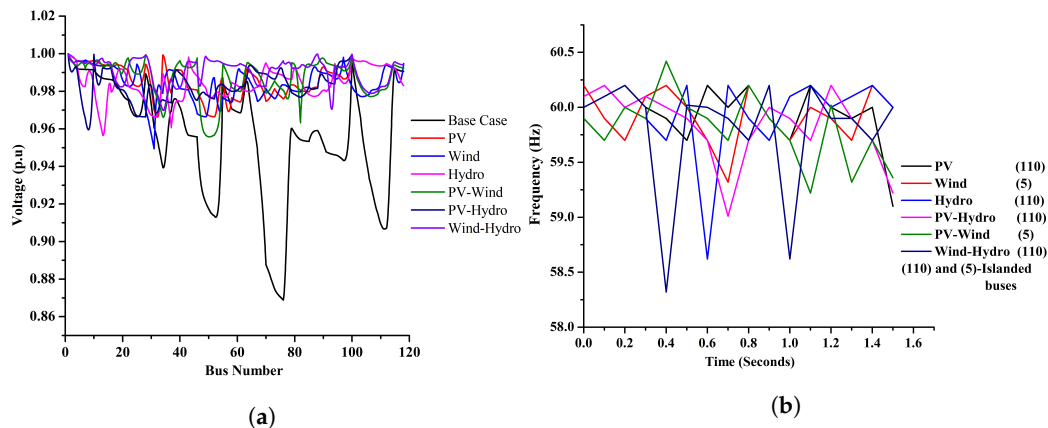


Figure 6. Voltage and frequency values. (a) Values (Voltage)-118 bus system. (b) Values (Frequency)-118 bus system.

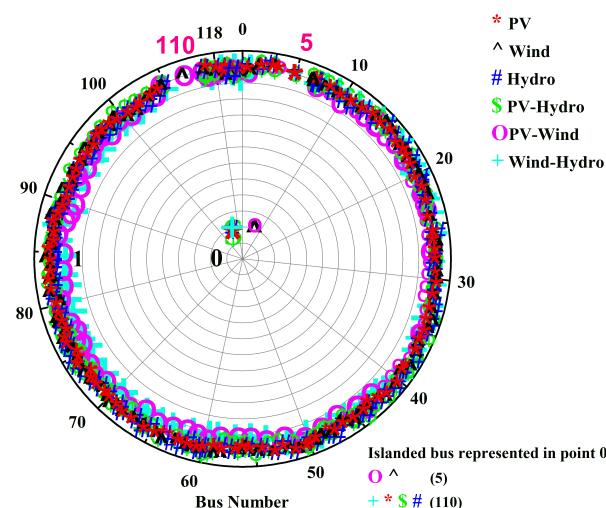


Figure 7. Detection of islanded buses-118 bus system.

3.2. Reconfiguration and Reliability Evaluation

The PSO technique is used for the reconfiguration. The identified vulnerable switch is opened and the remaining switches which must be opened without forming the loop to perform the reconfiguration. This ensures that the power loss is reduced and voltage profile is improved. The reliability analysis is performed for the IEEE-33 and 118 bus distribution system. Furthermore, the reconfiguration is performed for the vulnerable buses identified by the existing methods of islanding detection. The reliability indices after reconfiguration are calculated by selecting the global best solution with the fitness values using PSO. Each load of the system is considered to be an aggregated number of customers for evaluating the reliability indices.

3.2.1. Evaluation for the 33 Bus System

The reliability indices measurement of the 33 bus system using customer interruption is shown in Table 7. In this bus system, with the presence of distributed generation units, the islanded bus was identified by the proposed v&f index method.

Table 7. Comparison results of reliability evaluation for 33 bus system.

33 Bus System	Tie-Switches		Voltage Based Method [26]					Frequency Based Method [27]					Proposed Passive Method (Simultaneous Measurement of v&f Variation)				
			ENS	AENS	SAIDI	SAIFI	ASAI	ENS	AENS	SAIDI	SAIFI	ASAI	ENS	AENS	SAIDI	SAIFI	ASAI
Base case	33, 34, 35, 36, 37		27,622.03	1315.33	0.74	3.07	1.94	23508.5	1175.4	0.90	4.0495	1.938	4757.41	182.977	0.35	0.945	1.714
Reconfiguration (PSO)	PV	7, 9, 14, 32, 37	23,622.03	1115.33	0.65	2.05	1.74	20508.5	975.4	0.75	3.0295	1.638	4037.41	165.977	0.30	0.545	1.310
	Hydro	7, 9, 14, 28, 32	23,544.01	1055.21	0.63	2.03	1.71	20495.3	972.1	0.72	3.0012	1.634	4021.32	162.877	0.27	0.524	1.312
	PV-Hydro	7, 9, 14, 28, 32	23,324.03	1032.01	0.61	2.01	1.69	20325.1	970.3	0.71	2.9911	1.532	4002.11	160.677	0.23	0.444	1.112
	Wind-Hydro	7, 9, 14, 32, 37	22,122.13	1011.09	0.57	1.98	1.57	20100.5	960.5	0.69	2.1121	1.501	3990.02	158.070	0.19	0.381	1.010

The islanded distribution system can be restored by performing a reconfiguration of the network. The network reconfiguration is performed by identifying the most vulnerable buses. For this 33-bus system, it is necessary to keep five switches open to ensure radiality of the system. The identified vulnerable switch is incorporated by replacing any one (as identified from the results shown in Table 7) of the switches in the opened switches of the bus system and the reliability indices are computed as per Equations (21) to (24). In this bus system, switches 7, 9, 14, 32, and 37 are opened for PV. Similarly, 7, 9, 14, 28, and 32 are opened for Hydro, 7, 9, 14, 28, and 32 are opened for PV-Hydro, and 7, 9, 14, 32, and 37 are opened for Wind-Hydro. The reliability indices are compared in the presence of different DG units with the islanded buses identified by the methods given in [26,27].

In base case topology, the ENS indices are improved by 82.77% and 79.76% using the proposed technique, as compared with the first existing technique [26] and second existing technique [27], respectively. Likewise, AENS indices are improved by 86.08% and 84.43% using the proposed technique compared with the first existing technique [26] and second existing technique [27], respectively; SAIDI indices are improved by 52.72% and 61.39% using the proposed technique compared with the first existing technique [26] and second existing technique [27], respectively; SAIFI indices are improved by 69.21% and 76.66% using the proposed technique compared with the first existing technique [26] and second existing technique [27], respectively; and ASAI indices are improved by 11.64% and 11.19% using the proposed technique compared with the the first existing technique [26] and second existing technique [27], respectively.

In the reconfigured topology with the presence of PV, ENS indices are improved by 82.90% and 80.31% with the proposed technique compared with the first existing technique [26] and second existing technique [27], respectively. Likewise, AENS indices are improved by 85.11% and 82.98% using the proposed technique compared with the first existing technique [26] and second existing technique [27], respectively; SAIDI indices are improved by 53.84% and 60.03% using the proposed technique compared with the first existing technique [26] and second existing technique [27], SAIFI indices are improved by 73.41% and 82.01% using the proposed technique compared with the first existing technique [26] and second existing technique [27] and ASAI indices are improved by 24.48% and 19.78% using the proposed technique compared with the first existing technique [26] and second existing technique [27], respectively.

In the reconfigured topology with the presence of Hydro, ENS indices are improved by 82.91% and 80.37% using the proposed technique compared with the first existing technique [26] and second existing technique [27], respectively. Likewise, AENS indices are improved by 84.56% and 83.24% using the proposed technique compared with the first existing technique [26] and second existing technique [27], SAIDI indices are improved by 57.14% and 62.78% using the proposed technique compared with the first existing technique [26] and second existing technique [27], SAIFI indices are improved by 74.18% and 82.54% using the proposed technique compared with the first existing technique [26] and second existing technique [27] and ASAI indices are improved by 23.27% and 19.70% using the proposed technique compared with the first existing technique [26] and second existing technique [27], respectively.

In the reconfigured topology with the presence of PV-Hydro, ENS indices are improved by 82.84% and 80.30% using the proposed technique compared with the first existing technique [26] and second existing technique [27], respectively. Likewise, AENS indices are improved by 84.43% and 83.44% using the proposed technique compared with the first existing technique [26] and second existing technique [27], SAIDI indices are improved by 62.29% and 67.67% using the proposed technique compared with the first existing technique [26] and second existing technique [27], SAIFI indices are improved by 77.91% and 85.15% using the proposed technique compared with the first existing technique [26] and second existing technique [27] and ASAI indices are improved by 34.20% and 27.41% using the proposed technique compared with the first existing technique [26] and second existing technique [27], respectively.

In the reconfigured topology with the presence of Wind-Hydro, ENS indices are improved by 81.96% and 80.14% using the proposed technique compared with the first existing technique [26] and second existing technique [27], respectively. Likewise, AENS indices are improved by 84.36% and 83.54% using the proposed technique compared with the first existing technique [26] and second existing technique [27], SAIDI indices are improved by 66.66% and 72.50% using the proposed technique compared with the first existing technique [26] and second existing technique [27], SAIFI indices are improved by 80.75% and 81.96% using the proposed technique compared with the first existing technique [26] and second existing technique [27] and ASAI indices are improved by 35.68% and 32.71% using the proposed technique compared with the first existing technique [26] and second existing technique [27], respectively.

3.2.2. Evaluation for the 118 Bus System

The reliability indices measurement of the 118 bus system using customer interruption is shown in Table 8. In this bus system, with the presence of distributed generation units the islanded bus has been identified by the proposed v&f index method.

For this 118-bus system, it is necessary to keep 15 switches open to ensure the radiality of the system. The identified vulnerable switch is incorporated by replacing any one (as identified from the results shown in Table 8) of the switches in the opened switches of the bus system and the reliability indices are computed as per Equation (21) to (24). In this bus system, switches 24, 27, 34, 40, 43, 52, 59, 72, 75, 96, 98, 110, 123, 130, and 131 are opened for PV. Similarly, 9, 23, 35, 43, 52, 60, 71, 74, 82, 96, 99, 110, 120, 122, and 131 are opened for Hydro, 23, 27, 33, 43, 53, 62, 72, 75, 123, 125, 126, 129, 130, 131, and 132 are opened for PV-Hydro, and 9, 23, 35, 43, 52, 60, 71, 74, 82, 96, 99, 110, 120, 122, and 131 are opened for Wind-Hydro. The reliability indices are compared in the presence of different DG units with the islanded buses identified by the methods given in [26,27].

In the base case topology, ENS indices are improved by 39.04% and 38.17% using the proposed technique compared with the first existing technique [26] and second existing technique [27], respectively. Likewise, AENS indices are improved by 59.06% and 56.40% using the proposed technique compared with the first existing technique [26] and second existing technique [27], respectively; SAIDI indices are improved by 48.64% and 34.48% using the proposed technique compared with the first existing technique [26] and second existing technique [27], respectively; SAIFI indices are improved by 96.01% and 95.96% using the proposed technique compared with the first existing technique [26] and second existing technique [27], respectively; and ASAI indices are improved by 33.50% and 32.10% using the proposed technique compared with the first existing technique [26] and second existing technique [27], respectively.

In the reconfigured topology with the presence of PV, ENS indices are improved by 35.93% and 35.68% using the proposed technique compared with the first existing technique [26] and second existing technique [27], respectively. Likewise, AENS indices are improved by 62.08% and 62.29% using the proposed technique compared with the first existing technique [26] and second existing technique [27], respectively; SAIDI indices are improved by 62.85% and 51.85% using the proposed technique compared with the first existing technique [26] and second existing technique [27], respectively; SAIFI indices are improved by 96.56% and 96.57% using the proposed technique compared with the first existing technique [26] and second existing technique [27] and ASAI indices are improved by 28.16% and 23.78% using the proposed technique compared with the first existing technique [26] and second existing technique [27], respectively.

Table 8. Comparison results of reliability evaluation for the 118 bus system.

118 Bus System		Voltage Based Method [26]					Frequency Based Method [27]					Proposed Passive Method (Simultaneous Measurement of v&f Variation)				
		ENS	AENS	SAIDI	SAIFI	ASAI	ENS	AENS	SAIDI	SAIFI	ASAI	ENS	AENS	SAIDI	SAIFI	ASAI
Basecase		29,951.8	683.16	0.37	3.51	1.94	29,532.3	641.5	0.29	3.47	1.90	18,257.15	279.64	0.19	0.14	1.29
Reconfiguration (PSO)	PV	28,341.9	579.36	0.35	3.20	1.74	28,231.3	582.5	0.27	3.21	1.64	18,157.14	219.64	0.13	0.11	1.25
	Hydro	25,620.03	572.33	0.29	2.97	1.62	25,422.3	593.3	0.23	2.99	1.52	16,727.3	167.97	0.10	0.09	1.21
	PV-Hydro	20,142.13	553.21	0.25	2.96	1.59	20,025.1	480.3	0.21	2.97	1.50	8102.11	163.677	0.07	0.06	1.09
	Wind-Hydro	20,002.01	551.01	0.23	2.16	1.56	20,000.1	477.2	0.20	2.86	1.49	8011.21	149.544	0.04	0.03	1.06

In the reconfigured topology with the presence of Hydro, ENS indices are improved by 34.71% and 34.20% using the proposed technique compared with the first existing technique [26] and second existing technique [27], respectively. Likewise, AENS indices are improved by 70.65% and 71.68% using the proposed technique compared with the first existing technique [26] and second existing technique [27], respectively; SAIDI indices are improved by 65.51% and 56.52% using the proposed technique compared with the first existing technique [26] and second existing technique [27], respectively; SAIFI indices are improved by 96.96% and 96.98% using the proposed technique compared with the first existing technique [26] and second existing technique [27] and ASAI indices are improved by 25.30% and 20.39% using the proposed technique compared with the first existing technique [26] and second existing technique [27], respectively.

In the reconfigured topology with the presence of PV-Hydro, ENS indices are improved by 59.77% and 59.44% using the proposed technique compared with the first existing technique [26] and second existing technique [27], respectively. Likewise, AENS indices are improved by 70.41% and 65.92% using the proposed technique compared with the first existing technique [26] and second existing technique [27], respectively; SAIDI indices are improved by 72% and 66.66% using the proposed technique compared with the first existing technique [26] and second existing technique [27], respectively; SAIFI indices are improved by 97.97% and 97.97% using the proposed technique compared with the first existing technique [26] and second existing technique [27] and ASAI indices are improved by 31.44% and 27.33% using the proposed technique compared with the first existing technique [26] and second existing technique [27], respectively.

In the reconfigured topology with the presence of Wind-Hydro, ENS indices are improved by 59.94% and 59.94% using the proposed technique compared with the first existing technique [26] and second existing technique [27], respectively. Likewise, AENS indices are improved by 72.86% and 68.66% using the proposed technique compared with the first existing technique [26] and second existing technique [27], respectively; SAIDI indices are improved by 82.60% and 80% using the proposed technique compared with the first existing technique [26] and second existing technique [27], respectively; SAIFI indices are improved by 98.61% and 98.95% using the proposed technique compared with the first existing technique [26] and second existing technique [27] and ASAI indices are improved by 32.05% and 28.85% using the proposed technique compared with the first existing technique [26] and second existing technique [27], respectively.

4. Conclusions and Future Scope

The IEEE-33 and 118 electrical bus systems have been analyzed with various DG units. The islanding may occur due to sudden deviation in voltage and frequency at several buses. From the above system results, it is deduced that the proposed v&f index (passive islanding) method is effective for accurate detection of the islanded bus. In the existing methods, the voltage (v) violation and frequency (f) violation are studied separately, which leads to Non-Detection Zone. In the proposed v&f index (passive islanding) method, the changes of voltage and frequency are studied simultaneously, which minimizes the Non-Detection Zone and helps to identify the accurate islanded bus. Furthermore, the proposed method detects the islanded buses quicker than the existing methods and the number of islanded buses are lesser than the existing techniques.

The reliability of the system is improved by altering the topology of the system through reconfiguration. The reconfiguration is performed after detection of the vulnerable buses for islanding by the proposed v&f index (passive islanding) method. In the first stage, the reliability indices of the base case topology are considered. In this stage, the reliability indices of the system identified by different islanding detection techniques are evaluated. In the second stage, the reliability indices of base case topology are compared with the reliability indices in the presence of different DGs by a particular method of islanding detection. In the third stage, the reliability indices of a particular topology of reconfiguration are compared across different islanding detection methods. From these results, it was

found that the proposed islanding detection method in combination with the proposed reconfiguration method gives improved reliability of the system. This is due to the proper selection of switches to be opened by reconfiguration using PSO technique.

Due to operational conditions, the interruption cost (penalty) or lost profit from not supplied energy are not considered in this work, as the cost of electricity is not known. If the cost of electricity is known based on Real Time Price or Time of Use, this could be extended in the future.

Author Contributions: Conceptualization, S.R.; Methodology & Writing, S.R. and N.K.; Writing—original draft, N.K.; review & editing, G.S.; Supervision, P.N.B. All authors have read and agreed to the published version of the manuscript.

Funding: This research received no external funding.

Data Availability Statement: Not applicable.

Conflicts of Interest: The authors declare no conflict of interest

Abbreviations

DG	Distributed Generation
v&f	voltage and frequency
PSO	Particle Swarm Optimization
NDZ	Non-Detection Zone
ENS	Energy Not Supplied
SAIDI	System Average Interruption Duration Index
SAIFI	System Average Interruption Frequency Index
ASAI	Average Service Availability Index
BFS	Backward and Forward Sweep
AENS	Average Energy Not Supplied
N_{pan}	Number of panels
F_{fact}	Fill Factor
C_{volt}	Voltage coefficient
K_{curnt}	Current coefficient
O_{Power}	Output power
V_{pan}	Panel voltage
I_{pan}	Panel current
I_{MNPO}	The Maximum Net Power Output (MNPO) current
V_{MNPO}	The Maximum Net Power Output (MNPO) voltage
W_{rpow}	Power (Rated)
S_{rat}	Rated speed
C_{in}^{sp}	Speed (cut in)
C_{out}^{sp}	Speed (cut out)
ϵ_{Hy}	Hydraulic efficiency
ρ	Density
P_{he}	Effective pressure
g_{ac}	Acceleration
M_1 and M_2	v&f index and threshold
S_1 and S_2	The phase voltage related to time, frequency and voltage
$P_{lo(n)}$	(Real power) difference between first bus to next bus
$P_{alo(n)}$	Actual load
N_{smpl}	Samples (Range)
$V_{operating(N)}$	Operating voltage new
$V_{operating}$	Operating bus voltage
b_V	Voltage (base)
f_{ch}	Change in (f)-frequency
V_{ch}	Change in voltage
D_{fr}	Calculated frequency

n	Number of buses
G_b and $P_{(be)}$	global best solution and personal best solution
V_{ij}	particle velocity
F'	fitness value or objective function
y_i^{t+1}	specific place of the particle
(K_1)	acceleration constant
r_{1j}^t	random numbers
n_j	customer interruption or customer not served
h_j	customer hours available services
λ_j	failure rate
n_t	total number of customer served
$L_{b(j)}$	total demand

References

- Selim, A.; Kamel, S.; Mohamed, A.A.; Elattar, E.E. Optimal Allocation of Multiple Types of Distributed Generations in Radial Distribution Systems Using a Hybrid Technique. *Sustainability* **2021**, *13*, 6644. [\[CrossRef\]](#)
- Mohamed, A.A.; Kamel, S.; Selim, A.; Khurshaid, T.; Rhee, S.B. Developing a Hybrid Approach Based on Analytical and Metaheuristic Optimization Algorithms for the Optimization of Renewable DG Allocation Considering Various Types of Loads. *Sustainability* **2021**, *13*, 4447. [\[CrossRef\]](#)
- Ji, X.; Zhang, X.; Zhang, Y.; Yin, Z.; Yang, M.; Han, X. Three-Phase Symmetric Distribution Network Fast Dynamic Reconfiguration Based on Timing-Constrained Hierarchical Clustering Algorithm. *Symmetry* **2021**, *13*, 1479. [\[CrossRef\]](#)
- Shahid, M.U.; Alquthami, T.; Siddique, A.; Munir, H.M.; Abbas, S.; Abbas, Z. RES Based Islanded DC Microgrid with Enhanced Electrical Network Islanding Detection. *Energies* **2021**, *14*, 8432. [\[CrossRef\]](#)
- Lopez, J.R.; Ibarra, L.; Ponce, P.; Molina, A. A Decentralized Passive Islanding Detection Method Based on the Variations of Estimated Droop Characteristics. *Energies* **2021**, *14*, 7759. [\[CrossRef\]](#)
- Abokhalil, A.G.; Awan, A.B.; Al-Qawasmi, A.R. Comparative Study of Passive and Active Islanding Detection Methods for PV Grid-Connected Systems. *Sustainability* **2018**, *10*, 1798. [\[CrossRef\]](#)
- Bukhari, S.B.A.; Mehmood, K.K.; Wadood, A.; Park, H. Intelligent Islanding Detection of Microgrids Using Long Short-Term Memory Networks. *Energies* **2021**, *14*, 5762. [\[CrossRef\]](#)
- Montoya, O.D.; Arias-Londoño, A.; Grisales-Noreña, L.F.; Barrios, J.Á.; Chamorro, H.R. Optimal Demand Reconfiguration in Three-Phase Distribution Grids Using an MI-Convex Model. *Symmetry* **2021**, *13*, 1124. [\[CrossRef\]](#)
- Bakhshi-Jafarabadi, R.; Sadeh, J.; Rakhshani, E.; Popov, M. High power quality maximum power point tracking-based islanding detection method for grid-connected photovoltaic systems. *Int. J. Electr. Power Energy Syst.* **2021**, *131*, 107103. [\[CrossRef\]](#)
- Yafaoui, A.; Wu, B.; Kouro, S. Improved active frequency drift anti-islanding detection method for grid connected photovoltaic systems. *IEEE Trans. Power Electron.* **2011**, *2*, 2367–2375. [\[CrossRef\]](#)
- Ma, J.; Mi, C.; Zheng, S.; Wang, T.; Lan, X.; Wang, Z.; Thorp, J.S.; Phadke, A.G. Application of voltage harmonic distortion positive feedback for islanding detection. *Electr. Power Compon. Syst.* **2013**, *41*, 641–652. [\[CrossRef\]](#)
- Somalwar, R.; Kadwane, S.G.; Mohanta, D.K. Harmonics-based enhanced passive islanding method for grid-connected system. *Electr. Power Compon. Syst.* **2017**, *45*, 1554–1563. [\[CrossRef\]](#)
- Zarei, M.; Zangeneh, A. Multi-objective optimization model for distribution network reconfiguration in the presence of distributed generations. *Int. Trans. Electr. Energy Syst.* **2017**, *V27*, e2425. [\[CrossRef\]](#)
- Mohammadzadeh Niaki, A.H.; Afsharnia, S. A new passive islanding detection method and its performance evaluation for multi-DG systems. *Electr. Power Syst. Res.* **2014**, *110*, 180–187. [\[CrossRef\]](#)
- Sivanagaraju, S.; Visali, N.; Sankar, V.; Ramana, T. Enhancing voltage stability of radial distribution systems by network reconfiguration. *Electr. Power Compon. Syst.* **2005**, *V33*, 539–550. [\[CrossRef\]](#)
- Awad, A.S.A.; El-Fouly, T.H.M.; Salama, M.M.A. Optimal distributed generation allocation and load shedding for improving distribution system reliability. *Electr. Power Compon. Syst.* **2014**, *42*, 576–584. [\[CrossRef\]](#)
- Cheng, S.; Wei, Z.; Shang, D.; Zhao, Z.; Chen, H. Charging Load Prediction and Distribution Network Reliability Evaluation Considering Electric Vehicles' Spatial-Temporal Transfer Randomness. *IEEE Access* **2020**, *8*, 124084–124096. [\[CrossRef\]](#)
- He, J.; Guan, X. Uncertainty sensitivity analysis for reliability problems with parametric distributions. *IEEE Trans. Reliab.* **2017**, *6*, 712–721. [\[CrossRef\]](#)
- Jikeng, L.; Xudong, W.; Ling, Q. Reliability evaluation for the distribution system with distributed generation. *Eur. Trans. Electr. Power* **2011**, *21*, 895–909. [\[CrossRef\]](#)
- Dong, W.; Li, S.; Zhang, H.; Yu, X.; Hu, T. Sensitivity-based reliability coordination for power systems considering wind power reserve based on hybrid correlation control method for wind power forecast error. *Int. Trans. Electr. Energy Syst.* **2020**, *30*, e12307. [\[CrossRef\]](#)

21. Zhu, T.X. A new methodology of analytical formula deduction and sensitivity analysis of EENS in bulk power system reliability assessment. In Proceedings of the 2006 IEEE PES Power Systems Conference and Exposition, Atlanta, GA, USA, 29 October–1 November 2006; pp. 825–831.
22. Angel, A.R.; Manuel, S.A.-A. Design optimization for reliability improvement in microgrids with wind–tidal–photovoltaic generation. *Electr. Power Syst. Res.* **2020**, *188*, 106540.
23. Paterakis, N.G.; Mazza, A.; Santos, S.F.; Erdinç, O.; Chicco, G.; Bakirtzis, A.G.; Catalão, J.P.S. Multi-objective reconfiguration of radial distribution systems using reliability indices. *IEEE Trans. Power Syst.* **2015**, *31*, 1048–1062. [[CrossRef](#)]
24. Soroudi, A.; Aien, M.; Ehsan, M. A probabilistic modeling of photo voltaic modules and wind power generation impact on distribution networks. *IEEE Syst. J.* **2011**, *6*, 254–259.
25. Bhandari, B.; Poudel, S.R.; Lee, K.-T.; Ahn, S.-H. Mathematical modeling of hybrid renewable energy system: A review on small hydro-solar-wind power generation. *Int. J. Precis. Eng.-Manuf.-Green Technol.* **2014**, *1*, 157–173. [[CrossRef](#)]
26. Abd-Elkader, A.G.; Saleh, S.M.; Eiteba, M.B.M. A passive islanding detection strategy for multi-distributed generations. *Int. J. Electr. Power Energy Syst.* **2018**, *99*, 146–155. [[CrossRef](#)]
27. Narayanan, K.; Siddiqui, S.A.; Fozdar, M. Hybrid islanding detection method and priority-based load shedding for distribution networks in the presence of DG units. *IET Gener. Transm. Distrib.* **2017**, *11*, 586–595.
28. Nikhil, G.; Anil, S.; Niazi, K.R. Distribution network reconfiguration for power quality and reliability improvement using Genetic Algorithms. *Int. J. Electr. Power Energy Syst.* **2014**, *54*, 664–671.
29. Reddy, A.V.S.; Reddy, M.D. Optimization of network reconfiguration by using Particle swarm optimization. In Proceedings of the 2016 IEEE 1st International Conference on Power Electronics, Intelligent Control and Energy Systems (ICPEICES), Delhi, India, 4–6 July 2016; pp. 1–6.
30. Reddy, C.R.; Reddy, K.H. Islanding Detection Techniques for Grid Integrated Distributed Generation—A Review. *Int. J. Renew. Energy Res.* **2019**, *9*, 2.
31. Mathworks. *Matlab*, 2016b; Mathworks: Natick, MA, USA, 2016.
32. Prakash, D.B.; Lakshminarayana, C. Multiple DG placements in distribution system for power loss reduction using PSO Algorithm. *Procedia Technol.* **2016**, *25*, 785–792. [[CrossRef](#)]
33. Pottukkannan, B.; Suvarchala, K.; Muthukannan, P.; Thangaraj, Y. Optimal Allocation of Renewable Distributed Generation in Radial Distribution Network. *J. Adv. Res. Dyn. Control. Syst.* **2018**, *10*, 11.
34. Jamil, M.R.; Sun, Y.; Faisal, A.N.; Haes, A.H.; Siano, P.; Shafie-khah, M. A novel combined evolutionary algorithm for optimal planning of distributed generators in radial distribution systems. *Appl. Sci.* **2019**, *9*, 3394. [[CrossRef](#)]
35. Fang, X.; Li, F.; Wei, Y.; Azim, R.; Xu, Y. Reactive power planning under high penetration of wind energy using Benders decomposition. *IET Gener. Transm. Distrib.* **2015**, *9*, 1835–1844. [[CrossRef](#)]

Disclaimer/Publisher’s Note: The statements, opinions and data contained in all publications are solely those of the individual author(s) and contributor(s) and not of MDPI and/or the editor(s). MDPI and/or the editor(s) disclaim responsibility for any injury to people or property resulting from any ideas, methods, instructions or products referred to in the content.